

## Regular Article

# The effects of polar excipients transcitol and dexpanthenol on molecular mobility, permeability, and electrical impedance of the skin barrier



Sebastian Björklund<sup>a,b,\*</sup>, Quoc Dat Pham<sup>c</sup>, Louise Bastholm Jensen<sup>d</sup>, Nina Østergaard Knudsen<sup>d</sup>, Lars Dencker Nielsen<sup>d</sup>, Katarina Ekelund<sup>d</sup>, Tautgirdas Ruzgas<sup>a,b</sup>, Johan Engblom<sup>a,b</sup>, Emma Sparr<sup>c</sup>

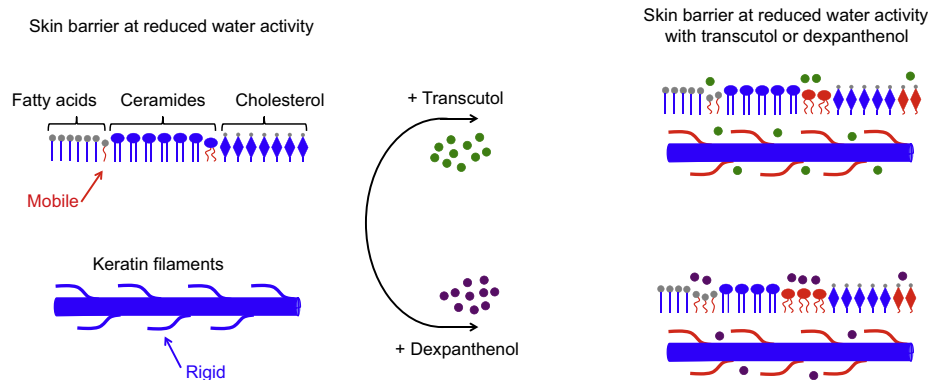
<sup>a</sup> Department of Biomedical Science, Faculty of Health and Society, Malmö University, SE-205 06 Malmö, Sweden

<sup>b</sup> Biofilms Research Center for Biointerfaces, Malmö University, SE-205 06 Malmö, Sweden

<sup>c</sup> Physical Chemistry, The Center for Chemistry and Chemical Engineering, Lund University, Box 124, SE-221 00 Lund, Sweden

<sup>d</sup> LEO Pharma A/S, Industriparken 55, DK-2750 Ballerup, Denmark

## GRAPHICAL ABSTRACT



## ARTICLE INFO

## Article history:

Received 15 April 2016

Revised 21 June 2016

Accepted 21 June 2016

Available online 23 June 2016

## Keywords:

Molecular mobility  
Skin permeability  
Steady-state flux  
Stratum corneum  
Topical drug delivery  
Excipients

## ABSTRACT

In the development of transdermal and topical products it is important to understand how formulation ingredients interact with the molecular components of the upper layer of the skin, the stratum corneum (SC), and thereby influence its macroscopic barrier properties. The aim here was to investigate the effect of two commonly used excipients, transcitol and dexpanthenol, on the molecular as well as the macroscopic properties of the skin membrane. Polarization transfer solid-state NMR methods were combined with steady-state flux and impedance spectroscopy measurements to investigate how these common excipients influence the molecular components of SC and its barrier function at strictly controlled hydration conditions *in vitro* with excised porcine skin. The NMR results provide completely new molecular insight into how transcitol and dexpanthenol affect specific molecular segments of both SC lipids and proteins. The presence of transcitol or dexpanthenol in the formulation at fixed water activity results in increased effective skin permeability of the model drug metronidazole. Finally, impedance spectroscopy data show clear changes of the effective skin capacitance after treatment with transcitol or dexpanthenol. Based on the complementary data, we are able to draw direct links between effects on the

\* Corresponding author at: Department of Biomedical Science, Faculty of Health and Society, Malmö University, SE-205 06 Malmö, Sweden.

E-mail address: [sebastianbjorklund@gmail.com](mailto:sebastianbjorklund@gmail.com) (S. Björklund).

molecular properties and on the macroscopic barrier function of the skin barrier under treatment with formulations containing transcitol or dexpanthenol.

© 2016 The Authors. Published by Elsevier Inc. This is an open access article under the CC BY-NC-ND license (<http://creativecommons.org/licenses/by-nc-nd/4.0/>).

## 1. Introduction

The outermost layer of skin is called the stratum corneum (SC) and constitutes the main barrier towards both inward and outward diffusional transport [1]. The barrier properties of SC are assured by its organization of dead keratin-filled cells, corneocytes, embedded in an extracellular matrix of lipid arranged in a multilamellar structure [2–4]. Although SC normally experience low relative humidity (RH), the exposure to very dry environments can lead to defective skin conditions, such as dry skin with reduced barrier function [5]. The continuous hydration of SC from the inside of the body, driven by the water gradient between the water-rich tissue and the surrounding environment, is consequently one crucial parameter for maintaining healthy skin [6,7]. In many cases of dry and defective skin, it is common to use topical formulations containing excipients and/or active substances that have beneficial effects on skin health. Considering this, the influence of hydration on the SC is particularly relevant for the optimization of topical formulations for treatment of skin diseases. Skin hydration is important both in relation to the state of the skin disease, as well as to the molecular organization of the skin lipid and protein components, and the partitioning and diffusion of drugs and excipients in the SC matrix. In many cases the degree of skin hydration is altered by topical treatment with a formulation, and it is well known that changes in skin hydration can lead to changes in skin permeability [8–10]. In previous studies, we have demonstrated that changes of a gradient in water activity across the skin can be used as a switch to regulate the skin permeability to different model drugs in a reversible manner [11]. This effect was later correlated to reversible structural and dynamical changes of the SC lipid or protein components [12–14]. It was found that increased SC hydration leads to mobilization of the non-aqueous SC components, associated with increased solubility and lowered diffusional resistance to external chemicals, for example, drugs or excipients in a formulation [11–13,15].

A common treatment of skin disease is topical application of a pharmaceutical product in which the active drug ingredient represents a minor fraction of the total formulation, while the excipients comprise the major part. Usually the excipients include, for example, solvents, penetration enhancers, and humectants, and all these compounds can have large impact on the treatment and the progression of the skin disease [16]. Therefore the topical formulation has to be optimized by considering how different excipients interact within the formulation, as well as with the lipid and protein components of the skin. In this analysis, it is important to consider both the molecular and the macroscopic effects caused by the topical formulation in order to gain a fundamental understanding of

how the skin barrier is influenced. This evaluation should also consider how the applied formulation influences the skin hydration. In order to distinguish the effects of certain formulation components from the overall effect of the formulation on skin hydration, it is desirable to make the comparisons to reference samples of the skin at the same water activity. All these important issues are considered in the present study, where we investigate how the excipient molecules transcitol, TC, and dexpanthenol, DexP, (see Fig. 1) influence the mobility of SC molecular components and the SC barrier function at controlled hydration conditions.

The present experimental approach is based on previous studies where the molecular effect of small polar molecules, such as urea and glycerol, was linked to their effects on the skin barrier function [17,18]. Similar to urea and glycerol, both TC and DexP are used in commercial skincare products. Urea and glycerol are also naturally present in skin as part of the so-called Natural Moisturizing Factor (NMF), which comprise a mixture of small polar molecules, such as free amino acids and their derivatives. The presence of NMF substances is considered crucial to maintain SC hydration in dry conditions [19]. Further, the effect of urea and glycerol on diseased skin has been emphasized *in vivo*, where formulations containing these substances reduce dryness [20,21]. From recent *in vitro* studies it was shown that urea and glycerol increase the molecular mobility of both SC lipids and proteins at moderate relative humidity where the SC components are considerably more rigid in the absence of these compounds, and it is notable that this effect could not be attributed to increased SC water content [18]. Considering that TC and DexP are small (i.e. low molecular weight) and polar and therefore have similar physicochemical properties as urea, glycerol, and other NMF substances, it is of basic relevance to investigate how these excipient molecules influence the molecular and macroscopic properties of the skin barrier in comparison to these previously investigated substances.

From an application perspective, TC is a safe and well tolerated solvent used in many cosmetic and pharmaceutical products for skin where its ability to dissolve poorly soluble substances is a clear benefit [22]. Likewise, DexP is found in many cosmetic products with the aim to increase the skin hydration and maintain skin softness, possibly due to its hygroscopic properties [23]. It has also been proposed that DexP can improve wound healing by activating fibroblast proliferation and accelerating the regeneration of the epidermal barrier [24,25]. However, a detailed understanding of the molecular interactions of TC and DexP with the protein and lipid molecular components of SC is lacking [22,26]. Also, the mechanism of TC and DexP on skin hydration and skin permeability is poorly understood. These aspects are addressed in the present paper where polarization transfer solid-state NMR methods

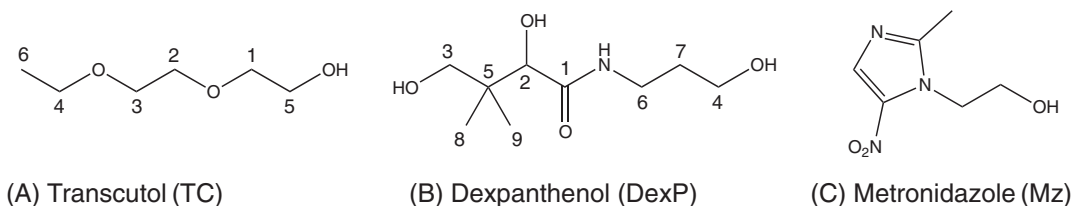


**Fig. 1.** Chemical structures of transcitol (TC), dexpanthenol (DexP), and the model drug metronidazole (Mz). A and B show labels of carbon resonances from the excipient molecules with numbers given according to their NMR chemical shifts (web: <http://sdfs.riodb.aist.go.jp>, National Institute of Advanced Industrial Science and Technology).

are combined with steady-state flux and impedance spectroscopy measurements to investigate how TC and DexP influence the molecular components of SC and its barrier function at strictly controlled hydration conditions. The experiments are performed in vitro with excised porcine skin. For the steady-state flux experiments the model drug metronidazole (Mz) is used (Fig. 1C), which we have employed also in previous studies [11,17]. Mz is a relevant model drug as it is commercially used as an antibacterial drug for treatment of the skin disease rosacea. Based on the complementary data from NMR, impedance spectroscopy and steady-state flux measurements, we are able to draw direct links between effects on the molecular properties and on the macroscopic barrier function of the skin barrier under treatment with formulations containing TC or DexP.

## 2. Materials and methods

### 2.1. Materials

NaCl,  $\text{KH}_2\text{PO}_4$ ,  $\text{Na}_2\text{HPO}_4 \cdot 2\text{H}_2\text{O}$  (all p.a. grade), MeOH (chromasolv grade), trypsin from bovine pancreas (T9201,  $\geq 90\%$  protein), and metronidazole (Mz, M3761, analytical standard grade,  $M_w = 171 \text{ g mol}^{-1}$ ,  $\log P = -0.02$ ) were purchased from Sigma Aldrich. Transcutol (TC,  $M_w = 134 \text{ g mol}^{-1}$ ,  $\log P = -0.42$ , ph. Eur. grade) was purchased from BASF and dexpanthenol (DexP,  $M_w = 205 \text{ g mol}^{-1}$ ,  $\log P = -0.99$ , ph. Eur. grade) was obtained from Gattefossé. Phosphate buffered saline (PBS) was prepared from deionized water (130.9 mM NaCl, 5.1 mM  $\text{Na}_2\text{HPO}_4 \cdot 2\text{H}_2\text{O}$ , and 1.5 mM  $\text{KH}_2\text{PO}_4$ , pH = 7.4). All formulations containing Mz were prepared in PBS with varying concentrations of TC or DexP, thus ensuring that both the active and excipient molecules are uncharged. The concentration of Mz was adjusted based on solubility data to obtain approximately the same thermodynamic activity of Mz in all formulation.

### 2.2. Preparation of skin membranes and the stratum corneum (SC) samples

Pig ears were obtained from a local abattoir and stored at  $-80^\circ\text{C}$  until use. Skin from the inside of the outer ear was dermatomed (TCM 3000 BL, Nouvag) to obtain skin strips with  $\sim 0.5 \text{ mm}$  thickness. Circular skin membranes with a diameter of 1.6 cm were punched out to fit the diffusion cells. SC samples to be studied with NMR were prepared by placing dermatomed skin strips for approximately 12 h on filter paper soaked in 0.2 wt% trypsin in PBS. Next, sheets of SC were removed with forceps and thoroughly washed in PBS. In this step, care was taken to remove tissue not belonging to SC by rubbing the downside of the SC sheets with cotton tipped applicators followed by rinsing in PBS. In order to avoid complications due to biological variation SC sheets were collected from several individual ears and cut in small pieces and pooled in one batch from which all samples were prepared.

### 2.3. Polarization transfer solid-state NMR (PT ssNMR) measurements on SC

The influence of TC and DexP on the molecular dynamics in SC lipid and protein components was investigated by means of solid-state NMR. For this purpose, SC sheets were soaked in formulations for 8 h at  $32^\circ\text{C}$ . The formulations contained either TC or DexP (5 or 30 wt%) in PBS solution. The SC sheets were then carefully wiped with paper tissues to remove excess formulation and placed directly into the NMR inserts. As a reference, SC sheets were prepared in an identical manner in neat PBS solution with no added

TC or DexP. A comparison between the results from the reference sample and previously obtained results on SC sheets prepared in the same manner (i.e. soaked in PBS) [14] showed virtually identical spectra, thus demonstrating good reproducibility. In some experiments, SC sheets were equilibrated at  $32^\circ\text{C}$  in a desiccator at 93%RH (adjusted by  $2.02 \text{ mol kg}^{-1}$  NaCl aqueous solution), corresponding to similar water activity as the formulation with 30 wt% TC or DexP.

NMR experiments were performed on a Bruker Avance-II 500 NMR spectrometer, equipped with a Bruker Efree 4 mm MAS probe at  $^1\text{H}$  and  $^{13}\text{C}$  resonance frequencies of 500 and 125 MHz, respectively. The magic-angle spinning (MAS) frequency was set to 5 kHz. The temperature was  $32^\circ\text{C}$  and calibrated by methanol [27]. The CP (cross polarization) [28] and INEPT (insensitive nuclei enhanced by polarization transfer) [29] for  $^1\text{H}$ - $^{13}\text{C}$  polarization transfer are commonly used schemes to enhance  $^{13}\text{C}$  signal. By comparing the signal intensities acquired with CP, INEPT and DP (direct polarization), where the latter shows resonances from all carbon segments in the sample and is used as a reference, site-specific information about molecular mobility can be obtained. We denote the DP-CP-INEPT set of experiments PT ssNMR (Polarization Transfer solid-state NMR) [30,31] for brevity.  $^{13}\text{C}$  spectra were acquired under 68 kHz two-pulse phase modulation (TPPM)  $^1\text{H}$  decoupling [32] using a spectral width of 250 ppm and an acquisition time of 0.05 s.  $^1\text{H}$  and  $^{13}\text{C}$  hard pulses were applied at  $\omega_{\text{H/C}}/2\pi = 80 \text{ kHz}$ . Ramped CP was performed with the contact time 1 ms, the  $^{13}\text{C}$  nutation frequency 80 kHz and the  $^1\text{H}$  nutation frequency linearly ramped from 72 to 88 kHz. The delays  $\tau = 1.8 \text{ ms}$  and  $\tau' = 1.2 \text{ ms}$  were used in INEPT. 2048 scans per experiment were collected with 5 s recycle delay giving a total time of approximately 8 h for all 3 experiments. The  $^{13}\text{C}$  spectra were externally referenced to the methylene signal of solid  $\alpha$ -glycine at 43.7 ppm. The data were processed with line broadening of 10 Hz, zero-filling from 1597 to 8192 time-domain points, Fourier transform, automatic phase correction [33], and baseline correction in Matlab using in-house code, partially derived from matNMR [34].

### 2.4. Adjustments of drug activity in the model formulations

We aim at formulations with different concentrations of the excipients (i.e. TC or DexP) but constant Mz activity in order to relate the observed differences in model drug flux across the skin membrane to changes caused by the excipients. To accomplish this we followed the procedure from previous studies [11,17]. In brief, the solubility of Mz was determined in neat PBS solution and in mixtures of TC or DexP in PBS solution. This was performed by mixing 3 g of formulation with excess Mz and stirring the saturated solution for 3 days in water-tight vials at  $32^\circ\text{C}$ . Three replicates of each formulation were prepared. The saturated suspensions were then filtered through  $0.2 \mu\text{m}$  syringe filters ( $\varnothing = 13 \text{ mm}$ , PTFE membranes, VWR), discarding the first part of the filtrate. Next, the saturated solutions were diluted appropriately before analysis (20  $\mu\text{l}$  filtrate to 50 mL PBS). The final step was repeated one time for all replicate formulations ( $n = 6$ ). The results are summarized in Table S1. Statistical outliers of the Mz solubility were excluded based on a two sided Grubbs' test at  $p = 0.05$ . The solubility limit of Mz equals the concentration corresponding to maximum activity (Fig. S1). After determining the solubility in each formulation, the concentration of Mz was adjusted to a determined concentration below the solubility limit to avoid precipitation of Mz, which can occur when handling close to saturated formulations. Here, the concentration of Mz in the solution of neat PBS was chosen to match the concentration used in commercial products that contains 0.75 wt% ( $7.5 \text{ mg mL}^{-1}$ ), which corresponds to 60% of the saturation concentration of Mz in PBS (Table S1). The factor of 0.6 was then consistently used to set the

actual concentration to obtain approximately the same Mz activity in all formulations. For clarity, the adjusted concentrations of Mz in all formulations are compiled in Table S1.

### 2.5. Water activity in the model formulations

Water activity was measured for all formulations ( $n = 2$ ) using a NovaSina LabMaster- $a_w$  apparatus at 32 °C. The instrument was calibrated with saturated salt solutions (83.6 and 97.0%RH) and milli-Q water (close to 100%RH) before measurements. The formulations were allowed to reach thermal equilibrium and then a stable value was recorded for a minimum period of 30 min. The results are compiled in Fig. S2, showing that the water activity decreases linearly with the molar concentration of the solute, irrespective of the type of solute (i.e. TC or DexP). The water activity in the same donor formulations was again measured after the diffusion experiments. A change in water activity would imply that there is a significant change in composition of the donor formulation over time during the experiment. The conclusion from these control experiments is that the water activity remained approximately constant (less than 1.5% change) during the diffusion-cell experiments.

### 2.6. Flow-through diffusion cell experiments

Diffusion experiments were performed with a flow-through cell set-up, which enables automatic sampling from 15 diffusion cells ( $\varnothing = 0.90$  cm) [35,36]. The cells are kept in a heater block connected to a circulating water bath (Techne TE-10A Thermoregulator), ensuring a constant temperature of 32 °C, and placed on top of a magnetic stirrer (Multipoint 15 Magnetic Stirrer, Variomag) with mixing of both the receptor and donor solutions at 200 rpm. The receptor phase was degassed at reduced pressure for approximately 1 h before starting the experiment to minimize formation of air bubbles under the membranes. The membranes were hydrated by placing them in the diffusion cells with flowing receptor solution for approximately 1 h before applying 2 mL of formulation (this procedure was not executed for membranes included in the impedance study, see below). The receptor solution was pumped (Ismatec IPC-16) through the system with a flow rate of 1.5 mL h<sup>-1</sup>. Directly after applying the formulations, the donor compartments were sealed with parafilm to avoid evaporation of water. Fractions of receptor solution were collected (Gilson FC 204 Fraction collector) in 2 h intervals during 24 h, starting from the time when the donor formulation was applied.

The data from the diffusion experiments were analyzed from curves of cumulative mass permeated per membrane area as a function of time. Data are presented as the steady-state flux ( $\mu\text{g cm}^{-2} \text{h}^{-1}$ ) across the skin membrane, which was determined from the slope of the linear region of the curve that corresponds to steady-state conditions. For this analysis, 5 data points between 16 and 24 h were used (see Fig. S3 for example of data). Statistical outliers in the data of the steady-state fluxes were excluded based on a two sided Grubbs' test at  $p = 0.05$ . The choice of time intervals was justified by the time required to reach steady-state flux, and this time is influenced by the water activity in the donor formulation [11]. To ensure steady-state conditions, we aim at constant composition of the donor and receptor phases during the course of the experiment. Therefore, the donor solution was applied in excess (i.e. 2 mL). Further, the receptor solution was continuously renewed by the flow-through set-up to assure low concentration of Mz in the receptor phase. Control measurements showed no major changes in the water activity in the donor solutions before and after the experiments, thus implying that the composition of the donor solutions remains virtually unchanged over the period of the experiment. Moreover, the total amounts of Mz ( $n = 54$ ),

TC ( $n = 7$ ) and DexP ( $n = 7$ ) that reached the receptor phase by the end of the experiment were determined. The amount of Mz in the receptor solution was 0.31% of the total amount in the donor solution, while the corresponding value for TC was determined to 0.45%. The measured concentration of DexP in the receptor solution by the end of the experiment was below the limit of detection ( $100 \mu\text{g g}^{-1}$ ), which implies slow diffusion of this substance from the donor solution across the skin membrane. The amount of Mz, TC or DexP that was dissolved in the skin membrane was not investigated.

### 2.7. Analytical procedures

In the solubility study, the concentration of Mz was determined by UV spectrophotometry (Cary 50, Varian Inc.). No signs of absorbance from TC or DexP were observed between 200 and 800 nm, while the wavelength of maximum absorbance for Mz was determined to 319 nm and used for quantification. The concentration of Mz was calculated from calibration curves of standard solutions with known concentrations (1, 2.5, 5.0, 7.5, 10.0, 15.0, and 20.0  $\mu\text{g g}^{-1}$ ).

The concentration of Mz in the receptor phase was analyzed by reversed phase HPLC-UV. 20  $\mu\text{l}$  of receptor solution was injected using an automatic sample injector (Rainin Dynamax model AI-1A) with a 10  $\mu\text{l}$  injection loop. The mobile phase consisted of filtered and degassed methanol:phosphate buffer (10 mM  $\text{KH}_2\text{PO}_4$ ) (20:80 v/v). The flow rate was set to 2.0 mL min<sup>-1</sup> (Varian 9012 solvent delivery system). A C<sub>18</sub> column (pore size = 120 Å, particle size = 5  $\mu\text{m}$ , dimensions = 50 × 4.6 mm i.d.) was used in series with an external guard holder equipped with C<sub>18</sub> guard cartridges (pore size = 120 Å, particle size = 5  $\mu\text{m}$ , dimensions = 10 × 4.0 mm i.d.). The retention time for Mz detection (Thermo Separation Products, Spectra 100) was 1.9 min.

The concentration of TC and DexP in the receptor phase was analyzed by gas chromatography mass spectrometry (GC/MS). An Agilent 7000 GC triple quad MS (Agilent Technologies) operated in MS scan mode ( $m/z$  50–650) was used. 1  $\mu\text{l}$  was injected into the multimode inlet (50 °C, 600 °C min<sup>-1</sup> to 200 °C). The injected sample was separated on a 30 m × 0.25 mm i.d. capillary column coated with 0.25  $\mu\text{m}$  stationary phase, BPX 50 (Scientific glass Engineering, SGC part no. 054751) using temperature gradient programming (50 °C for 2 min followed by 20 °C min<sup>-1</sup> to 250 °C). The carrier gas was helium at a flow of 1.2 mL min<sup>-1</sup>. The transfer line into the mass spectrometer was maintained at 280 °C. The analytes were detected by electron ionization (EI, 70 eV). Reference solutions of TC (1, 5, 10, 50, and 100  $\mu\text{g mL}^{-1}$ ) were prepared in PBS and linearity was demonstrated for this concentration range. The TC concentration was determined from the response of the 10  $\mu\text{g mL}^{-1}$  reference solution using the external standard principle. Samples from experiments where the formulations contained 5 wt% TC were diluted 10 times with water prior to injection. In the corresponding case where the formulations contained 30 wt% TC, the samples were diluted 100 times. The retention time for TC was 4.6 min and the run time was set to 12 min. The EI mass spectrum was confirmed by comparison with corresponding spectra from the NIST 11 MS library database. Two injections were carried out for each sample solution. Reference solutions were injected multiple times throughout the sequence. The concentration of DexP was below the detection limit for all receptor solution samples investigated.

### 2.8. Impedance spectroscopy on skin membranes

Electrical impedance measurements were performed with a Franz cell ( $\varnothing = 0.90$  cm,  $V = 6$  mL, PermeGear Inc.) equipped with four electrodes connected to a potentiostat from Ivium

Technologies; (see Fig. S4A). Platinum wires were employed as working and counter electrodes, while Ag/AgCl/3M KCl electrodes (World Precision Instruments) were used as sensing and reference electrodes. The frequency range was set from 1 MHz to 0.5 Hz with 7 frequencies per decade, which resulted in a total measuring time of less than 1 min. The amplitude of the applied voltage was set to 25 mV ensuring low current densities in the lower frequency range. The water jacket was kept at 32 °C by a circulating water bath (Techne TE-10A Thermoregulator).

Initial impedance scans were measured on skin membranes that had been hydrated for approximately 1–2 h by placing them on filter paper soaked in PBS at room temperature. Next, the membranes were placed in the flow-through diffusion cells for determination of the Mz steady-state flux as described above. After the diffusion experiments, the membranes were taken from the flow-through diffusion cells and placed on a filter paper soaked in PBS. Finally, the membranes were sequentially mounted in the Franz cell for the final impedance measurements. Both initial and final measurements were conducted by placing the skin membrane on top of the receptor chamber with the dermal side facing the receptor solution, which consisted of degassed PBS. Then the donor chamber was clamped on top of the receptor chamber and filled with degassed PBS solution. For each set of experiment (i.e. initial or final impedance measurements) the time difference between the first and last measurement was less than 60 min. The impedance experiments were designed with consideration of the natural variability in skin membrane impedance previously reported [37–39]. Our experimental design circumvents this natural variability as it generates experimental data from the same membrane before and after being in contact with the applied model drug formulation.

For analysis of the skin impedance data we employed a model circuit (Fig. S4B), consisting of a resistor (solution resistance,  $R_{sol}$ ) in series with a parallel arrangement of a resistor (skin membrane resistance,  $R$ ) and a constant-phase element (CPE). This circuit is frequently used for analyzing skin impedance data [14,40–42]. The resistance values were obtained from the real part of the impedance in the frequency regions where the imaginary part gives minimum contribution to the total impedance. For  $R_{sol}$ , this region corresponds to high frequencies in the range of  $\sim 0.2$ – $0.1$  MHz. In average,  $R_{sol} = 134 \pm 4 \Omega$  ( $\pm$ SEM) including all measurements ( $n = 60$ ). The corresponding frequency region for the membrane resistance  $R$  occurs at low frequencies close to direct current (DC) where  $R = Z_{re} - R_{sol}$ . In this analysis, all data were normalized with the skin membrane area ( $0.64 \text{ cm}^2$ ) to get units in  $\Omega \text{ cm}^2$ .

The heterogeneous and complex nature of skin membranes result in deviations from ideal properties, which is consistent with several impedance studies on skin [14,40,41,43]. This issue is accounted for by the empirical CPE element, which can be used to derive an effective capacitance  $C_{eff}$  of the SC [44]. For this, we followed a procedure in which the SC layers are considered to have a distribution of varying time-constants in the vertical direction across the skin membrane [40]. The effective capacitance  $C_{eff}$  was derived from the high frequency region from the imaginary impedance data following a graphical representation method, which does not involve any fitting [44]. The procedure used to calculate  $C_{eff}$  from the impedance spectroscopy data is described in detail in the supplementary text with examples of raw data (cf. Figs. S5–S9). In addition, all impedance data from the initial and final measurements are compiled in Table S2.

### 3. Results

We employ solid-state NMR methods that enable detailed characterization of the effect of TC and DexP on the SC molecular

components under varying hydration conditions. The effect of the same excipient compounds on the skin barrier function is investigated at similar hydration conditions. In addition, we performed impedance measurements before and after the steady-state diffusion experiments to investigate the effect of TC and DexP on the electrical resistance and capacitance of the skin membrane.

#### 3.1. Molecular mobility in SC components as revealed from PT ssNMR

PT ssNMR [30,31] was recently successfully employed on intact SC to characterize molecular dynamics in individual segments of SC lipid and protein components [13,14,18]. The experiments are based on natural-abundance  $^{13}\text{C}$  solid-state NMR and involves MAS (magic angle spinning) and heteronuclear decoupling to minimize peak broadening from CSA (chemical shift anisotropy) and heteronuclear scalar and dipolar couplings to obtain chemical shift resolution of  $^{13}\text{C}$  molecular segments. Information on the molecular dynamics is obtained by comparing the signal intensities from the INEPT (insensitive nuclei enhanced by polarization transfer) and CP (cross polarization) pulse sequences, relative to the signal obtained in the DP (direct polarization) experiment. INEPT is normally used to enhance the signal in liquid state NMR [29], while CP is a corresponding standard scheme employed in solid-state NMR [28]. The DP experiment does not involve polarization transfer and the DP signal intensity may thus be used as a reference in comparison to the INEPT and CP signal intensities. The INEPT and CP signals from a specific resolved segment will depend on its dynamical properties, which may be defined in terms of mobility or rigidity. The distinction between rigid and mobile molecular segments is rationalized by the relation between the experimental DP, INEPT, and CP signal intensities with respect to the theoretical signal intensity ratios, as described in detail by Topgaard et al. [30]. In brief, the INEPT and CP signal intensities vary as a function of the rotational correlation time ( $\tau_c$ ) and the  $^{13}\text{C}$ – $^1\text{H}$  bond order parameter  $S_{\text{CH}}$ , from which it is possible to distinguish different dynamic regimes [30]. The correlation time  $\tau_c$  measures the rate of the  $^{13}\text{C}$ – $^1\text{H}$  bond reorientations, while the order parameter  $S_{\text{CH}}$  quantifies the time-averaged orientation of the  $^{13}\text{C}$ – $^1\text{H}$  bond with respect to a main symmetry axis (for example the normal axis of a lipid bilayer) and is thus a measure of anisotropy. Both the INEPT and the CP pulse sequences transfer magnetization from  $^1\text{H}$  nuclei to neighboring  $^{13}\text{C}$  and enhance the resonance signals depending on the dynamical properties of the molecular segments. The polarization transfer occurs in different ways, and this is taken advantage of in PT ssNMR for selective signal enhancement of mobile or rigid molecular segments. For INEPT, the transfer of magnetization occurs via through-bond scalar couplings that act in favor for signal enhancement of mobile segments with isotropic motion. For CP the transfer of polarization occurs via through-space dipolar interactions, which is fast for rigid segments with anisotropic reorientations leading to efficient signal enhancement in these cases.

A detailed peak assignment of most  $^{13}\text{C}$  resonances of intact SC was previously obtained by comparing spectra from extracted SC protein and lipid components and model lipids [13]. Based on this peak assignment we investigated the effect of TC and DexP on the mobility (fluidity) of SC molecular components by PT ssNMR. Representative data, obtained from sheets of isolated SC that were soaked in either solutions of PBS with added TC or DexP (0, 5 or 30 wt%), are shown in Fig. 2. The complex composition of SC is reflected in the crowded  $^{13}\text{C}$  NMR spectra, which show overlaid DP (grey), CP (blue), and INEPT (red) spectra from the SC samples. Relevant “signature peaks” from the protein and lipid components for intact SC are labeled in Fig. 2A. The Gly  $C_{\alpha}$  ( $\sim 44$  ppm), Ser  $C_{\alpha}$  ( $\sim 57$  ppm), and Ser  $C_{\beta}$  ( $\sim 62$  ppm) peaks are most relevant for characterizing the mobility of the keratin filaments due to their generally high abundance in keratin (approximately 40% of the total

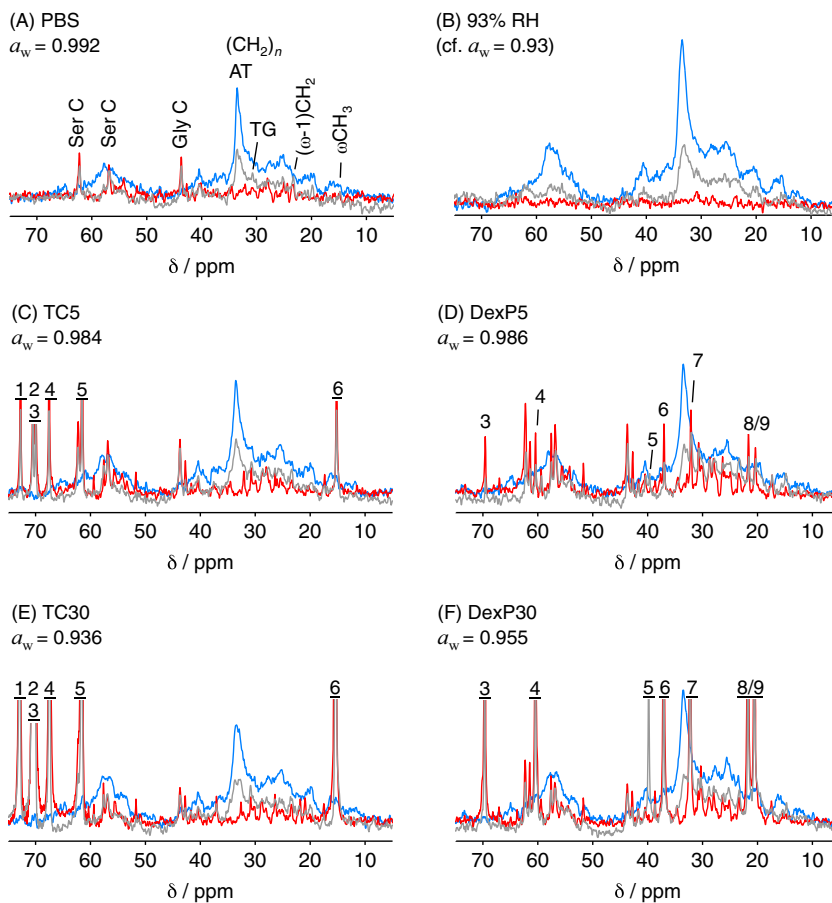


**Fig. 2.** PT ssNMR  $^{13}\text{C}$  spectra (DP in grey, CP in blue, INEPT in red) from SC sheets treated for 8 h in neat PBS or formulations containing either 5 or 30 wt% transcutool (TC) or dexpanthenol (DexP). Resonances from prominent protein and lipid molecular components are labeled in spectra (A), corresponding to SC in neat PBS. (B) shows spectra from SC sheets equilibrated at 93%RH after being soaked in neat PBS for 8 h. The peaks from TC are labeled according to Fig. 1 in spectra (C) and (E), while the resonances from DexP are labeled in (D) and (F). In all cases, sample treatment and NMR experiment were performed at 32 °C. The signal intensity is equal in all spectra. (For interpretation of the references to colour in this figure legend, the reader is referred to the web version of this article.)

amino acid residues of keratin K1 and K10 are glycine or serine) [13]. In particular, the N- and C-terminal domains of the keratin filaments are highly enriched in glycine and serine [13]. The lipid carbons represent a minor fraction of the total number of carbons in SC. However, most of the SC lipids are saturated and have long hydrocarbon chains in the range of C14–C32 [45,46]. The majority of these carbons resonates at similar chemical shifts, which compensate for the fact that the lipid carbons represent a minor fraction. The methylene groups  $(\text{CH}_2)_n$  with all-trans (AT) conformation resonate at  $\sim 33$  ppm, while methylene groups exhibiting a distribution of trans/gauche (TG) conformers resonate at  $\sim 31$  ppm [47]. In addition to the main methylene carbon peaks, the terminal carbons of the lipid chains,  $\omega\text{CH}_3$  ( $\sim 15$  ppm) and  $(\omega - 1)\text{CH}_2$  ( $\sim 23$  ppm), can be used as markers for the SC lipids.

Both TC and DexP can be distinguished in the NMR spectra in Fig. 2, and the assignments of the carbon resonances from these molecules are indicated. The signal intensity from the excipient molecules increases with their concentration in the solution used to equilibrate the SC samples. The DP signal is fairly quantitative in the dynamical regimes where INEPT gives signal [30], which is here the case. It is therefore possible to estimate the relative amounts of TC and DexP molecules in SC from the signal intensity in the NMR spectra. By comparing the DP signal intensity of the carbon resonances from the excipient molecules in Fig. 2, we estimate that the sample treated in 30 wt% TC contains  $5.5 \pm 0.3$  times more TC as compared to the sample treated in 5 wt%. The corresponding number for the samples treated in DexP is  $6.5 \pm 2.2$ .

These estimations indicate that the partitioning of the excipient molecules into the SC samples is close to proportional to their concentration in the PBS formulation. It is further noted that the resonances from the excipient molecules are characterized with prominent INEPT signal and no CP contribution, implying that these excipient molecules are present in the SC samples in a mobile state.

In all spectra in Fig. 2, the CP signal from rigid SC molecular segments is dominating (excluding the INEPT contribution from the excipient carbons). The high CP signal intensity indicates that the main fraction of the SC components is in a rigid state. The most prominent lipid CP peak is found for the all-trans  $(\text{CH}_2)_n$  resonances at 33 ppm, while the broad CP peak centered at 57 ppm is mainly ascribed to  $\text{C}_\alpha$  resonances of the peptide bond from all amino acid residues (except Gly  $\text{C}_\alpha$ ). For most of the spectra in Fig. 2, several resonances are also characterized with distinct INEPT signal, which implies that a small fraction of the SC protein and lipid components is mobile under these conditions.

The general conclusion from the data in Fig. 2 is that the overall behavior of SC lipid and proteins is similar for the SC samples treated in solutions of pure PBS or solutions with TC or DexP. It was previously shown that the molecular dynamics in SC components strongly depend on its hydration [13,48,49], which can be expressed in terms of thermodynamic water activity (ranging between zero and unity). When the SC sample is equilibrated in an excess aqueous solution with given solute composition, or with vapor with given RH, the water activity in the SC sample will reach

the same value of water activity as the water activity in the excess solution/vapor phase (see Ref. [14] for example). To take the effect of hydration into account when evaluating the present data, we measured the water activity in all formulations used (Table S1, Fig. S2), and relevant values are indicated in Fig. 2. The water activity is clearly reduced with increasing concentration of the excipients. To enable comparisons of the effect of the excipients at similar water activities, we included also data for a SC sample that was first soaked in the PBS solution and thereafter equilibrated at 93%RH (Fig. 2B). The latter set of data differs from all other spectra in Fig. 2 in that it shows no strong INEPT signals for any lipid or protein segment (Fig. 2B). It is a striking observation that the SC samples treated with TC or DexP show similar behavior as the fully hydrated SC sample (Fig. 2A) even though the water activity is reduced by the addition of excipients. From a more detailed analysis of the spectra in Fig. 2, small variations in the INEPT enhancement due to the treatment of different formulations can be detected, and this will be analyzed below.

### 3.2. The effect of TC and DexP on molecular dynamics in SC lipid components

Fig. 3A and B show carbon resonances corresponding to relevant lipid and cholesterol molecular segments to enable a detailed comparison between the spectra from SC samples treated with neat PBS or different formulations containing either TC or DexP. We first focus on the chemical shift from the methylene groups in the lipid chains (Fig. 4A), where the DP spectrum displays one peak centered around 33 ppm for rigid acyl chains with all-trans conformation, and one smaller peak centered around 31 ppm for more disordered acyl chains with a distribution of trans/gauche conformers [47]. Furthermore, it is seen that the peak around 33 ppm is selectively more enhanced in the CP spectrum, while the peak around 31 ppm is more enhanced in the INEPT spectrum, showing that a small fraction of methylene carbons undergoes fast reorientation between the conformations. The presence of TC and DexP in the SC results in more intense INEPT signal (relative to DP) from trans-gauche (TG) resonances in comparison to the SC that was treated in neat PBS, implying slightly higher mobility in the SC lipids. This effect is most pronounced in the SC sample treated with the solution containing 5 wt% DexP. Still, it should be pointed out that the prominent CP peak from the all-trans configured acyl chains is similar for all samples, which implies that the main fraction of lipids remain in a rigid all-trans configuration in all conditions investigated.

From a detailed investigation of the spectra in Fig. 2 several prominent INEPT peaks were identified and assigned to resonances from ceramide and cholesterol carbons [13,50]. For clarity, we present close-ups of the peaks corresponding to these carbons,

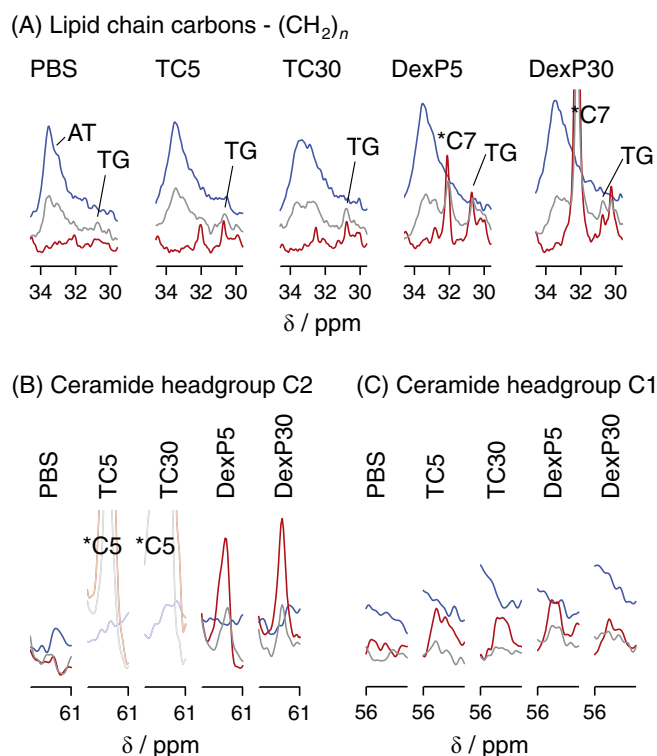


**Fig. 4.** PT ssNMR  $^{13}\text{C}$  spectra (DP in grey, CP in blue, INEPT in red) in close-up showing resonances from (A) lipid chain methylene groups  $(\text{CH}_2)_n$  and (B and C) ceramide headgroup segments. The signal is 3 times more intense in A and 1.3 times more intense in B and C, as compared to the intensity in Fig. 2. \*C7 and \*C5 in (A) and (B), respectively, indicate carbon resonances from the excipient molecules (cf. Fig. 1). (For interpretation of the references to colour in this figure legend, the reader is referred to the web version of this article.)

starting with ceramide resonances in Fig. 4B and C. Interestingly, the INEPT peaks from ceramide headgroup carbons [13,18] are more pronounced (relative to DP) in the spectra corresponding to the SC samples treated with TC or DexP, as compared to SC treated in neat PBS buffer. It is here noted that the peak corresponding to TC C5 (Fig. 4B) overlaps with the signal from the CER C2 resonance, which makes it impossible to draw any conclusions on how TC influences the mobility of this particular carbon segment. However, the presence of DexP clearly increases the INEPT signal from the CER C2 resonance in comparison to the spectra from the SC sample treated in PBS solution. This indicates that DexP increases the mobility of the ceramide C2 headgroup segment. In the close-up of the spectra from the CER C1 resonance, the INEPT signal is of moderate intensity for the spectra corresponding to the TC

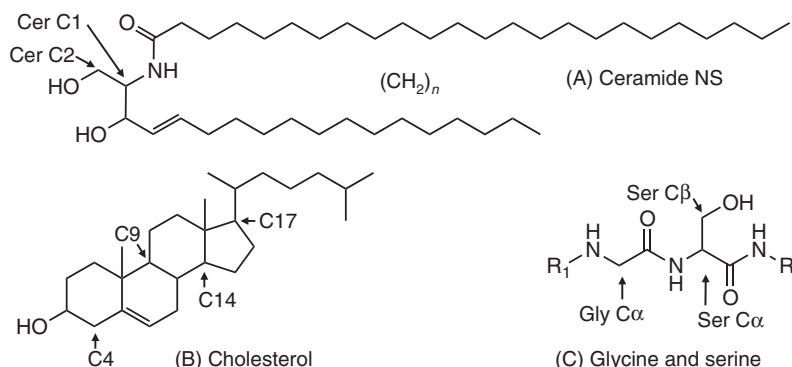


**Fig. 3.** Relevant lipid and protein molecular segments, here exemplified with (A) ceramide NS, (B) cholesterol, and (C) a peptide consisting of glycine and serine.

and DexP SC samples. Still, the INEPT signal is more enhanced as compared to the SC sample without the added excipients. It should be pointed out that the CER C1 resonance occurs in the chemical shift regime where several amino acid residues are expected to give signal from the  $C_{\alpha}$  of the peptide bond. Therefore, it is difficult to uniquely determine if the observed effects is only due to enhanced mobility in the CER C1, where the differences in ceramide headgroups (e.g. CER NS or NP) give rise to minor changes of the resonance frequency, or from enhanced mobility in both CER C1 and protein resonances from the peptide bond  $C_{\alpha}$ .

Similar effect of enhanced mobility as seen for the ceramide headgroups is also seen for cholesterol. From Fig. 5 it is clear that the INEPT intensity from several cholesterol carbons is enhanced when either TC or DexP is present in the SC sample. The most prominent effect is observed in the spectra corresponding to the SC sample treated with the solution containing 5 wt% DexP.

### 3.3. The effect of TC and DexP on molecular dynamics in SC protein components

The spectra corresponding to the SC sample treated in neat PBS solution (Fig. 2) show clear INEPT peaks from the Gly  $C_{\alpha}$ , Ser  $C_{\alpha}$ , and Ser  $C_{\beta}$  resonances; see Fig. 3C for the chemical structure of these molecular segments.

To enable more detailed comparisons, we present close-ups of the relevant chemical shifts in Fig. 6. It is shown that Gly  $C_{\alpha}$ , Ser  $C_{\alpha}$ , and Ser  $C_{\beta}$  resonances give rise to prominent INEPT signal in all spectra. This is consistent with increased mobility of the flexible N- and C-terminal domains of the individual protein chains in the keratin filaments. In general, these segments do not provide any CP

signal with similar line shape as the DP or INEPT peaks, which implies that these molecular segments are in the fast dynamic regime with isotropic reorientations. A more detailed comparison shows that the relation between the INEPT and DP signals in the spectra corresponding to the SC samples treated in neat PBS, 30 wt% TC, and 30 wt% DexP is very similar. In addition, the spectra corresponding to the SC samples treated in 5 wt% TC or DexP show a higher INEPT signal, relative to the DP signal. These findings suggest that the mobility of the keratin filament terminals is slightly increased in the case of SC treatment with 5 wt% of TC or DexP, as compared to treatment in solutions of neat PBS or PBS with 30 wt% of the excipients.

### 3.4. Steady-state flux of the model drug

The molecular information obtained with the solid-state NMR method can be related to the macroscopic effects of the same excipients on the SC barrier properties under similar hydration conditions. We investigated permeation of the model drug Mz across skin membranes in contact with solutions of the same composition as used in the NMR studies. The composition of the formulation can drastically influence the activity (chemical potential) of the drug molecule in the formulation, which in turn affects the release rate and the driving force for transport (the activity gradient across the membrane). To accomplish well-defined experimental conditions we adjusted the Mz activity to achieve similar thermodynamic activity of the drug in all formulations according to its solubility in the different solutions (see Fig. S1).

The mean values of the measured steady-state fluxes of Mz and TC across skin membranes are compiled in Table 1. The overall

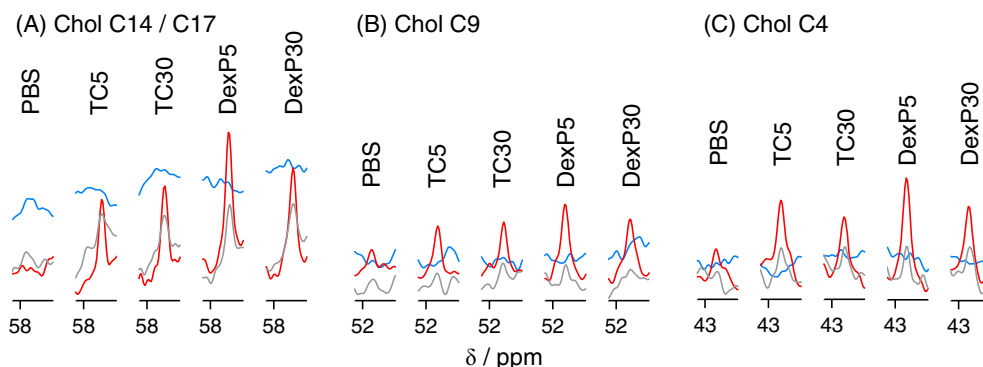


Fig. 5. PT ssNMR  $^{13}\text{C}$  spectra (DP in grey, CP in blue, INEPT in red) in close-up showing resonances from cholesterol segments. The signal is 3 times more intense as compared to the intensity in Fig. 2. (For interpretation of the references to colour in this figure legend, the reader is referred to the web version of this article.)

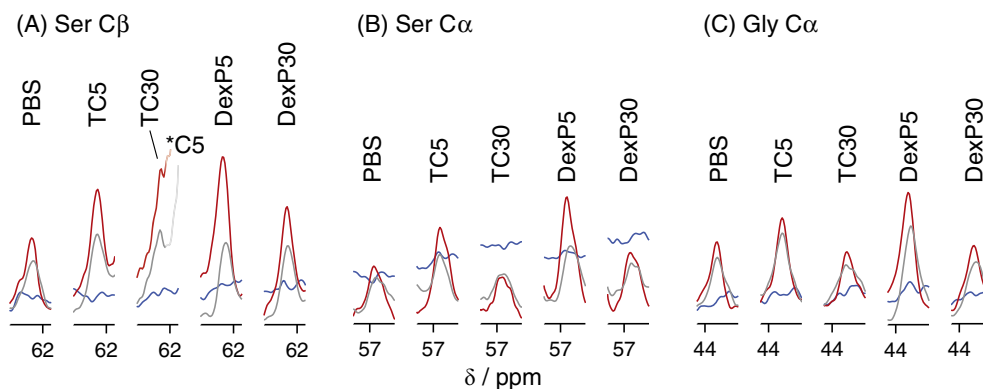


Fig. 6. PT ssNMR  $^{13}\text{C}$  spectra (DP in grey, CP in blue, INEPT in red) in close-up showing resonances from Ser  $C_{\beta}$ , Ser  $C_{\alpha}$ , and Gly  $C_{\alpha}$  segments. The signal is 2 times more intense as compared to the intensity in Fig. 2. C5 in (A) indicate a resonance from TC (cf. Fig. 1). (For interpretation of the references to colour in this figure legend, the reader is referred to the web version of this article.)



**Table 1**

Steady-state flux ( $J_{ss}/\mu\text{g cm}^{-2} \text{h}^{-1}$ ) of Mz, TC, and DexP across skin membranes (example of data are shown in Fig. S3). Deviations are given by the standard error of the mean ( $\pm\text{SEM}$ ). LOD is limit of detection. The measured water activity ( $a_w$ ) in the formulations is also given.

Formulation <sup>a</sup>	$J_{ss}$ (skin)			$a_w$
	Mz	TC	DexP	
PBS	$6.1 \pm 0.9$ (n = 12)	n.a.	n.a.	$0.992 \pm 0.002$ (n = 2)
TC5	$6.3 \pm 1.3$ (n = 10)	$55 \pm 11$ (n = 7)	n.a.	$0.984 \pm 0.002$ (n = 2)
TC30	$6.7 \pm 1.0$ (n = 12)	$231 \pm 40$ (n = 7)	n.a.	$0.936 \pm 0.000$ (n = 2)
DexP5	$6.9 \pm 1.3$ (n = 10)	n.a.	n.a.	$0.986 \pm 0.001$ (n = 2)
DexP30	$4.5 \pm 1.0$ (n = 10)	n.a.	<LOD (n = 7)	$0.955 \pm 0.001$ (n = 2)

<sup>a</sup> Abbreviations: TC - transcutol, DexP - dexpanthenol. Numbers give concentration in wt%.

conclusion is that the mean flux of Mz across the skin membranes is similar for all formulations. The only exception is found for the formulation that contains 30 wt% DexP, which gives slightly lower Mz flux. However, one-way ANOVA-analysis did not reveal any statistical difference between this formulation and the others (p-level 0.60). From Table 1, it is further concluded that the flux of TC increases with increasing concentration gradient (i.e., concentration in the donor solution), and the average value of the steady-state flux of TC is  $\sim 4$  times higher from the 30 wt% formulation, as compared to the formulation with 5 wt%. The corresponding comparison between the total cumulative mass of permeated TC is  $\sim 6$  times higher from the formulations with high concentration. With respect to the standard deviations for the flux it is thus reasonable to say that the TC flux is close to proportional to the TC concentration in the donor formulation. We finally note that the Mz flux does not vary significantly between the formulations with 5 or 30 wt% TC even though the formulations have different water activity and SC likely contain different amounts of TC in these cases. The corresponding analysis for permeation of DexP was not possible as the concentration in the receptor cell was below the limit of detection ( $\text{LOD} \approx 100 \mu\text{g mL}^{-1}$ ) even for the formulation with the highest concentration of DexP. It should here be noted that the method used for DexP analysis is less sensitive as compared to that used for TC analysis, and that a receptor concentration of DexP that is equal to LOD would correspond to a flux of approximately  $240 \mu\text{g cm}^{-2} \text{h}^{-1}$ , which is similar to the measured TC flux.

### 3.5. The effect of TC and DexP on skin permeability at reduced water activity

In the diffusion cell experiments, the water activity of the receptor solution is kept constant at physiological conditions ( $a_w \sim 0.992$ ), while the water activity of the donor solutions is

lower than 0.992 and depends on the concentration of TC or DexP (Table 1). The experimental set-up mimics in vivo conditions, where the water activity inside the body is constant at physiological conditions, while the outside atmosphere, a film of formulation, etc., can vary between dry and humid. In Fig. 7A, the experimental data are presented as the average Mz flux as a function of water activity in the donor cell. The results are compared to previously published data of Mz flux across skin in conditions where the water activity in the donor cell was regulated by the addition of various amounts of large water soluble polymers [11]. In the latter case, the polymers do not partition into the skin membrane [51,52], and only act to reduce the water activity, in analogue to so-called osmotic stress technique [53]. The main conclusion from Fig. 7A is that the steady-state Mz flux remains high at dehydrating conditions when the water activity is adjusted by the addition of TC or DexP, while there is a clear reduction in Mz flux when the water activity is adjusted by the addition of water-soluble polymers. This difference can be explained by the partitioning of the smaller molecules (TC or DexP) into the skin membrane where they influence its properties, while the relatively large polymers do not partition inside the membrane and thus only act to dehydrate the skin [51,52].

### 3.6. The effect of TC and DexP on the skin electrical properties

The studies of Mz permeation across skin were complemented with impedance measurements using the very same samples and conditions in terms of formulation composition. Experiments were performed prior and after the diffusion cell studies, and the data are summarized in Table 2. To minimize the contribution from the biological variability between different skin membranes, which is generally observed [14,37–39], we present the impedance results as the relative changes of  $R$  and  $C_{\text{eff}}$  by calculating the ratio

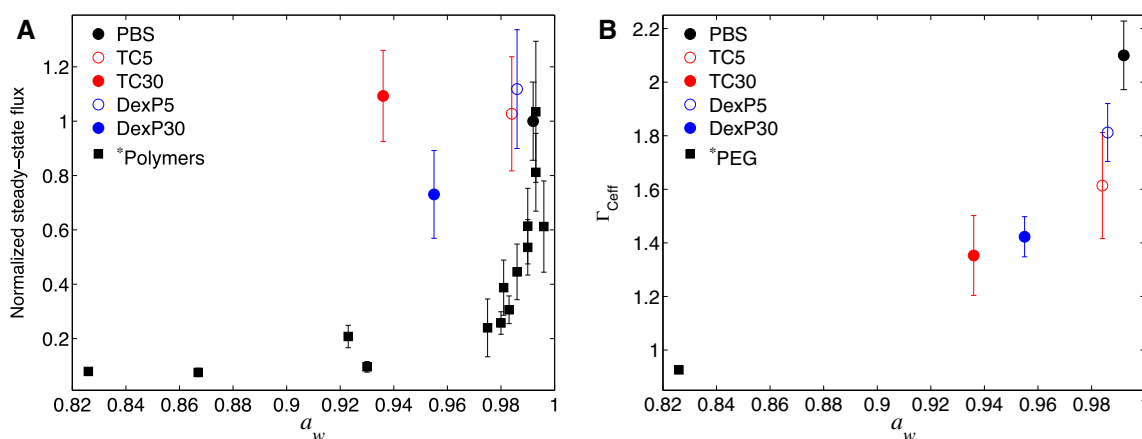


**Fig. 7.** (A) Normalized steady-state flux of Mz and (B) relative change of  $C_{\text{eff}}$  as a function of water activity ( $a_w$ ) in the donor formulation. Data in (A) are presented as the relative change in flux compared to the Mz flux from donor solution of neat PBS, while data in (B) show the ratio of the final and initial value of  $C_{\text{eff}}$ . Deviations are given by the standard error of the mean ( $\pm\text{SEM}$ ). \*Polymers show data from Ref. [11] and \*PEG shows data from Ref. [14].

**Table 2**

Relative change of  $R$ ,  $C_{\text{eff}}$  for skin membranes after 24 h exposure to the model drug formulations. The relative change is given by the mean value of the ratios between the final (f) and initial (i) values for each individual skin membrane (see Tables S2–S3 for the complete set of individual data). Deviations are given by the standard error of the mean ( $\pm$ SEM).

Formulation <sup>a</sup>	$\Gamma_R = \frac{R_f}{R_i}$	$\Gamma_{C_{\text{eff}}} = \frac{C_{\text{eff},f}}{C_{\text{eff},i}}$
PBS (n = 10)	0.13 $\pm$ 0.02	2.1 $\pm$ 0.1
TC5 (n = 5)	0.20 $\pm$ 0.06	1.6 $\pm$ 0.2
TC30 (n = 5)	0.22 $\pm$ 0.05	1.4 $\pm$ 0.2
DexP5 (n = 5)	0.15 $\pm$ 0.03	1.8 $\pm$ 0.1
DexP30 (n = 4)	0.70 $\pm$ 0.15	1.4 $\pm$ 0.1

<sup>a</sup> Abbreviations: TC - transcutol, DexP - dexpanthenol. Numbers give concentration in wt%.

of the final and initial values for each individual skin membrane (see Tables S2–S3 for the complete set of individual data). The overall conclusion is that  $R$  decreases during the diffusion experiments, while  $C_{\text{eff}}$  increases. For simplicity we denote the ratio between the final (f) and initial (i) values as  $\Gamma_x = \frac{y_f}{x_i}$ , where  $x$  is either  $R$  or  $C_{\text{eff}}$ . A more detailed comparison of the impedance data for the different formulations shows that there is no statistical difference between  $\Gamma_R$  corresponding to donor solutions of PBS, TC5, TC30, and DexP5 (p-level 0.28), while there is a significantly lower decrease in  $\Gamma_R$  for the case corresponding to DexP30 (p-level 0.00). Furthermore, the increase of  $\Gamma_{C_{\text{eff}}}$  is more pronounced for neat PBS and for the formulations with 5 wt% TC or DexP, as compared to the formulations containing 30 wt% TC or DexP.

The change of  $\Gamma_{C_{\text{eff}}}$  for the skin membranes treated with the different formulations are presented in Fig. 7B. The data are presented with respect to the variation in water activity in the donor solution. Strikingly, the results show a clear trend of stronger increase of  $C_{\text{eff}}$  for skin membranes exposed to formulations with high water activity. The results in Fig. 7B are compared to results from a previously reported impedance study on skin membranes where the water activity in the donor cell was regulated by the addition of water soluble polymers [14]. The reference data [14] show that  $C_{\text{eff}}$  of the skin membranes exposed to a formulation with relatively low water activity (i.e.  $a_w = 0.826$ , 65 wt% PEG 1500 Da) decreases slightly over the 24 h exposure time, which is in strong contrast to the present results. Taken together, the results is consistent with that  $C_{\text{eff}}$  is highly dependent on the SC hydration, which is controlled by the external water activity in the formulation [14]. The corresponding changes of  $\Gamma_R$  are presented in Fig. S10. In conclusion, the results show that both  $\Gamma_{C_{\text{eff}}}$  and  $\Gamma_R$  strongly depend on the water activity.

## 4. Discussion

### 4.1. Relating SC molecular and macroscopic properties

It is clear that changes of the structure and molecular dynamics of the SC protein and lipid components can have large impact on the macroscopic properties of the SC membrane, including its barrier properties, electrical resistance and capacitance characteristics, as well as material properties like strength and elasticity. Here, we aim to relate the observed effects of TC and DexP on SC barrier properties to the molecular effects induced by these excipients on the mobility of SC lipids and protein components. This aim was achieved by investigating the macroscopic barrier properties from steady-state flux and impedance measurements and relating these results to the molecular properties measured by solid-state NMR methods. The experiments were designed so that the skin

samples were treated with the same formulations under well-defined conditions in terms of water activity, thus enabling direct comparison of the results from the different experimental methods.

The first conclusion from the combined data presented here is that TC and DexP have no major effect on the SC permeability of Mz, as compared to the reference sample of (close to) fully hydrated SC treated in neat PBS buffer. However, this comparison neglects the fact that the different formulations do not have the same water activity. Previous studies have shown large changes in SC barrier function, SC electrical properties and molecular mobility in SC lipid and proteins for the corresponding range of water activities [6,11,13,14,48,49]. In the present study, the skin samples were treated in solutions with different amounts of excipients and at different water activities. In the analysis we need to consider the combined effects of SC dehydration and interactions between SC components and the added excipient molecules. In the comparison in Fig. 2 we therefore include the reference data for the neat SC at similar water activities as in the formulations (Figs. 2 and 7 and S10). The clear conclusion from this comparison is that both TC and DexP maintain the properties of hydrated SC also in slightly dehydrated conditions. The steady-state flux results can be understood on basis of the observations from the PT ssNMR experiments showing that the lipid chain carbons have similar mobility in all samples, independent on hydration degree (Fig. 4A). The same conclusion was previously drawn for skin membranes treated other small polar molecules, urea or glycerol, resulting in a retained and high skin permeability at dehydrating conditions [17]. Furthermore, detailed studies of the molecular mobility of SC lipid components and other lipid systems have shown that samples that contain urea or glycerol retain mobility similar to fully hydrated samples also in dehydrated conditions [18,54,55]. TC and DexP have similar physicochemical properties as urea, glycerol, and other NMF substances, and we propose that the same mechanism of retained molecular mobility of SC at dehydrating conditions act also for DexP and TC at corresponding situations.

A more detailed inspection of the NMR data reveals small variations in the molecular mobility of some protein and lipid segments (Figs. 4–6), which are more difficult to directly relate to the observed unchanged SC permeability to the model drug Mz. This might in part be explained by that the measurement precision in the diffusion cell studies is limited due to biological variations between skin samples. In principle, one can expect that increased fluidity in SC molecular components will lead to increased SC effective permeability. However, a deeper analysis of this connection between molecular properties and barrier function requires also information on arrangement of the mobile and rigid SC components in relation to the possible transport routes through skin. Typically, one expect that fluidizing the lipid hydrocarbon layers can provide additional routes for transport, or increase the size of existing ones, allowing for enhanced molecular transport across the layer. On the other hand, increased mobility in the plane of the polar headgroups of the bilayer likely has less impact on the overall permeability, as the main resistance to the flux lies in the rigid hydrocarbon chains of the lipid lamellae (cf.  $(\text{CH}_2)_n$  in Fig. 4A). This is highly relevant with respect to the present findings where the treatment with both TC and DexP caused increased mobility of the ceramide headgroup segments located at the interface of the bilayer (Fig. 4B and C) without leading to increased permeability of Mz across SC (Fig. 7A) due to similar mobility of the lipid chain carbons in all samples (Fig. 4A).

To explain the impedance results we can start by concluding that the SC samples treated in solutions with TC or DexP indeed have different solvent composition within the membrane as compared to the neat PBS buffer as the excipient molecules partitions

in the SC sample. In fact, the results in Fig. 2 show that the presence of these excipient molecules is proportional to the concentration of the formulation in contact with the SC membrane. In other words, even though the molecular mobility is similar in the different SC samples, it is reasonable that the electrical properties differ as the solvent composition inside the SC change. The dielectric properties of the capacitive domains are expected to change with the addition of the excipients, leading to a less pronounced increase of the effective membrane capacitance (assuming that the dielectric constant  $\epsilon$  (water)  $>$   $\epsilon$  (TC/DexP)) (Fig. 7B). This would be consistent with a preferential location of the excipient molecules in the interfacial headgroup regions of the extracellular lipid lamellae, where the capacitive domains are expected to be located [41,56–58]. From the NMR data we only observe the molecular consequences of adding certain molecules, and not their exact position in the SC matrix. Still, the observations of increased mobility in the ceramide headgroups (Fig. 4B and C) imply that the added excipient molecules have strong influence in this layer. This is also consistent with the log P values of  $-0.42$  and  $-0.99$  for TC and DexP, respectively, implying preferential partitioning in more polar environments, such as the headgroup region of the lipid lamellae.

#### 4.2. Molecular consequence of adding TC or DexP to intact SC

SC is a composite where the major fraction is composed of corneocytes (85 wt% in dry SC) [15]. The multilamellar lipid matrix, on the other hand, contains long hydrophobic lipids with very low water content [59]. When foreign compounds are added to SC, they partition between these regions on basis of their solubility in the different compartments. From the NMR experiments, we are able to distinguish between the molecular consequences of adding the excipients TC and DexP on the SC lipid and protein components.

The results in Figs. 4 and 5 show that the addition of TC and DexP to intact SC leads to an increase of the fluidity in several lipid and cholesterol segments, as compared to the neat SC that was treated in neat PBS solution. Likewise, Figs. 2 and 6 show that treatment of SC in neat PBS or in TC and DexP formulations leads to enhanced mobility of the glycine and serine residues, which are highly abundant in the terminal domains of the keratin filaments, as compared to the SC sample equilibrated in 93%RH that is associated with rigid protein segments. It was previously demonstrated using the same PT ssNMR method on intact SC that

the mobility of the terminal domains of the keratin filaments strongly decreases under dehydrating conditions [13,14] (Fig. 2B). This is in strong contrast to the present results (Figs. 2C–F and 6), which show that the addition of TC or DexP leads to high mobility in the terminal protein segments also in slightly dehydrated conditions.

For clarity, we summarize our interpretation of the NMR results in Fig. 8. The overall effect is fairly similar for both excipients and both concentrations investigated. When the SC is exposed to formulations with low water activity it experience dehydration, which in general leads to increased rigidity of the SC lipids and proteins [13,14]. The present results show that TC and DexP act to retain, or increase, the mobility of several SC lipid and protein segments in dehydrated conditions. This indicates that these excipient molecules interact with lipid segments of the extracellular lamellae and protein residues in the corneocytes in SC and thus compensate for reduced hydration by retaining/increasing molecular fluidity.

#### 4.3. The influence of TC or DexP on skin membrane resistance

The parameter  $R$  reflects the restriction of ion transport across the total SC, which includes both the isolated corneocytes and the continuous extracellular lipid lamellar structures. In this study we evaluate the skin membrane resistance in terms of the relative change  $\Gamma_R = \frac{R_f}{R_i}$  (see Table 2 and Fig. S10A). This ratio reveals how the formulations in contact with the skin membrane influences the membrane resistance relative to its initial value obtained before the treatment with the formulation. A first conclusion is that  $\Gamma_R$  decreases for all skin membranes, implying that all aqueous formulations investigated affect the skin membranes by decreasing the restriction of ion transport across the barrier. This is likely explained by increased hydration during the prolonged diffusion cell experiments, as compared to the initial hydration state of the membrane. When the skin membrane is exposed to a formulation with low water activity ( $a_w = 0.826$ ) the membrane resistance increases leading to a significantly higher value of  $\Gamma_R$  (see Fig. S10A). These changes of ion restriction should predominantly be related to hydration/dehydration induced lipid mobility in the extracellular continuous lamellae, while changes of mobility of the intracellular protein components upon hydration/dehydration only can influence the mobility of intracellular ions. Thus, the observed effect on  $R$  is in all cases dependent on the ability

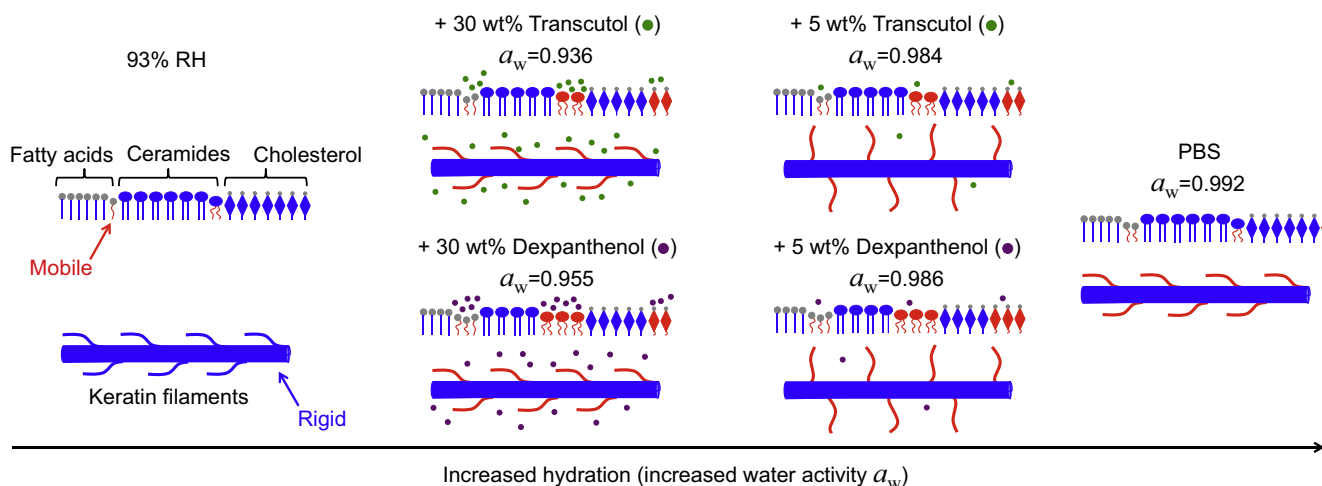


**Fig. 8.** Schematic interpretation of the molecular mobility of the SC protein (keratin filaments) and lipid components (fatty acids, ceramides, and cholesterol). Blue represents rigid molecular segments, while red represents mobile molecular segments. Grey indicates the unknown mobility in the headgroup of fatty acids and cholesterol. (For interpretation of the references to colour in this figure legend, the reader is referred to the web version of this article.)

of ions to cross the complete SC, where the extracellular lipids represents the main barrier [1], and this ability may be increased due to formation of more fluid regions in the bilayers (Figs. 4 and 5) where ions can diffuse with less restriction.

#### 4.4. The influence of TC or DexP on skin membrane capacitance

The impedance data show the strongest increase in  $C_{\text{eff}}$  for skin membranes in contact with the formulations having the highest water activities (see Fig. 7B). The SC capacitance has mainly been attributed to the dielectric nature of lipid structures that impede transport of ions in the SC membrane [41,56–58]. If  $C_{\text{eff}}$  is ascribed completely to the SC lipid lamellae then these domains can be visualized as dielectric medium in between the corneocytes. In this case, the capacitance ( $\text{F cm}^{-2}$ ) depends on the thickness,  $d$ , and the dielectric constant,  $\epsilon$ , of these domains, according to Eq. (1), where  $\epsilon_0$  is the permittivity of vacuum ( $8.9 \times 10^{-14} \text{ F cm}^{-1}$ ).

$$C_{\text{eff}} = \frac{\epsilon_0 \epsilon}{d} \quad (1)$$

The thickness  $d$  of the lipid lamellae has been demonstrated to be unaffected by hydration from X-ray diffraction studies on pig SC [14,60]. Thus, as a first approximation, an increase or decrease of  $\Gamma_{C_{\text{eff}}}$  can be explained by that the dielectric properties of the capacitive regions of SC change due to addition or removal of water molecules, respectively. This effect is clearly illustrated by the reference data in Fig. 7B (obtained with 65 wt% PEG 1500 Da), where the low water activity ( $a_w = 0.826$ ) leads to a slight decrease of  $\Gamma_{C_{\text{eff}}}$  due to dehydration [14]. The fact that  $\Gamma_{C_{\text{eff}}}$  is lower for the formulations containing higher amounts of excipients (i.e. lower water activities) in the donor formulation (Fig. 7B) can thus be explained by dehydration of the capacitive regions of SC. However, it is also likely that incorporation of TC or DexP into the capacitive regions results in lower values of  $\epsilon$ , based on the assumption that both TC and DexP have lower dielectric constants as compared to water. Taken together, it is likely that both these effects work in parallel leading to a clear reduction of  $\Gamma_{C_{\text{eff}}}$  at lower water activities (Fig. 7B).

#### 4.5. Implications to skin formulations

Studies like this can be used to increase the understanding of the impact of excipients on molecular properties of the skin to design and justify the choice and composition of excipients in a pharmaceutical formulation. When developing a formulation the thermodynamic activity of all components (including water) is important for the performance of the final product. Normally, the water activity in the viable epidermis is controlled at physiological conditions, while the water activity of the external environment is determined by the relative humidity in air (RH). When the SC is not exposed to any formulation, its hydration is thus determined by boundary conditions set by the underlying tissue and the surrounding vapor. However, when a formulation is applied onto the skin surface, the water activity in the outer surface of the skin is instead determined by the properties of the (drying) film of the formulation [61]. This change in boundary condition might indeed affect the properties of the skin barrier; for example, increased fluidity of the SC molecular components likely leads to increased SC effective permeability also at ambient hydration conditions. This reasoning highlights the importance of defining and controlling the water activity in topical formulations to maximize the beneficial effects of excipients and active ingredients with respect to diseased or dry skin.

It is shown here that TC and DexP can be used to control the skin permeability in relation to the external water activity. Extrapolated to a real situation, the results demonstrate how these excip-

ients may be used to generate the properties of a hydrated skin membrane also in dehydrated conditions. Water has a relatively high vapor pressure compared to most excipients in formulations. Therefore, these polar excipient molecules will be less affected by evaporation and stay on the skin application site in situations where water evaporates.

Another mechanism that may alter the skin permeation for foreign molecules is the excipient impact on the solubility in the skin matrix. The NMR experiments showed both TC and DexP to be in liquid state in the SC mixture, which suggests that they can alter the solubility of other components in the skin, and thereby affect the permeation. The impact of improved solubility in hydrated skin is most likely less pronounced for small hydrophilic molecules, such as Mz, as compared to small hydrophobic substances (in hydrated SC). In fact, TC has been suggested to increase the skin solubility of more lipophilic substances both in vitro and in vivo [62–64]. The present study provides completely new data showing that TC and DexP increase the molecular mobility of several lipid segments, which is likely the reason for increased skin solubility of more lipophilic substances [62–64].

## 5. Conclusions

In this work we investigate the effect of TC and DexP on the molecular mobility of SC components and on the macroscopic membrane properties, such as permeability and electrical characteristics. The use of complementary methods provides a novel tool to link molecular properties with macroscopic effects, and the results lead to deepened understanding of how these excipients influence lipid and protein components of the complex stratum corneum barrier membrane. We envisage that the experimental approach employed in this study is highly useful for future rational development of formulations for topical or transdermal drug delivery. The significance of the present results is highlighted in the following main conclusions:

- (i) Addition of TC or DexP leads to increased mobility of SC molecular components (i.e., both lipids and proteins) even though their presence acts to lower the water activity and thus impose dehydrating conditions.
- (ii) TC and DexP can be used to retain the high skin permeability of a hydrated membrane at reduced hydration conditions, which otherwise would lead to reduced flux due to dehydration induced molecular rigidity of the SC barrier components. This finding is explained by retained molecular mobility of SC at dehydrating conditions in the presence of TC and DexP.
- (iii) The presence of TC and DexP leads to increased mobility in the ceramide headgroups, which suggests that TC and DexP disturb the packing in the interfacial headgroup layer of lipid layers. Strikingly, the impedance results show a clear trend of stronger increase of  $C_{\text{eff}}$  for skin membranes exposed to formulations comprising TC and DexP and/or high water activity. This is consistent with a preferential location of the excipient molecules at the interfacial regions of the extracellular lipid lamellae, where the capacitive domains are expected to be located.
- (iv) TC has previously been suggested to increase the solubility of lipophilic substances in the skin [62–64]. The new observation of increased mobility of several lipid molecular segments after exposure to TC (and DexP) provides a likely explanation of increased skin solubility of lipophilic substances.
- (v) Urea and glycerol have clear effect on the mobility of SC lipid and protein components in dehydrated conditions [18], which can be related to increasing pliability and softness

of SC treated with these compounds under dry conditions [20]. TC and DexP have similar physicochemical properties as urea, glycerol, and other NMF substances, and we hypothesize that also these molecules influence the molecular dynamics of the SC in a similar manner.

## Acknowledgements

We thank Vitaly Kocherbitov from Malmö University and André Eriksson, Gitte Pommergaard Pedersen and Karsten Petersson from LEO Pharma A/S for fruitful discussions. The Swedish Research Council (VR) is also gratefully acknowledged for financial support both through regular grants (TR, ES, DP) and the Linnaeus Center of Excellence “Organizing molecular matter” (ES, DP). We furthermore thank the Swedish Foundation for Strategic Research (ES), the Crafoord Foundation (ES, DP), the Gustaf Th. Ohlsson Foundation (JE and TR) for financial support.

## Appendix A. Supplementary material

Supplementary data associated with this article can be found, in the online version, at <http://dx.doi.org/10.1016/j.jcis.2016.06.054>.

## References

- [1] R. Scheuplein, I.H. Blank, Permeability of skin, *Physiol. Rev.* 51 (4) (1971) 702–747.
- [2] K.C. Madison, D.C. Swartzendruber, P.W. Wertz, D.T. Downing, Presence of intact intercellular lipid lamellae in the upper layers of the stratum corneum, *J. Invest. Dermatol.* 88 (6) (1987) 714–718.
- [3] A. Weerheim, M. Ponc, Determination of stratum corneum lipid profile by tape stripping in combination with high-performance thin-layer chromatography, *Arch. Dermatol. Res.* 293 (4) (2001) 191–199.
- [4] E. Candi, R. Schmidt, G. Melino, The cornified envelope: a model of cell death in the skin, *Nat. Rev. Mol. Cell. Biol.* 6 (4) (2005) 328–340.
- [5] P. Garcia Ortiz, S.H. Hansen, V.P. Shah, T. Menne, E. Benfeldt, Impact of adult atopic dermatitis on topical drug penetration: assessment by cutaneous microdialysis and tape stripping, *Acta Derm. Venereol.* 89 (1) (2009) 33–38.
- [6] I.H. Blank, Further observations on factors which influence the water content of the stratum corneum, *J. Invest. Dermatol.* 21 (4) (1953) 259–271.
- [7] C.R. Harding, A. Watkinson, A.V. Rawlings, I.R. Scott, Dry skin, moisturization and corneodesmolysis, *Int. J. Cosmet. Sci.* 22 (1) (2000) 21–52.
- [8] T. Hikima, H. Maibach, Skin penetration flux and lag-time of steroids across hydrated and dehydrated human skin in vitro, *Biol. Pharm. Bull.* 29 (11) (2006) 2270–2273.
- [9] H. Zhai, I. Maibach Howard, Occlusion vs. skin barrier function, *Skin Res. Technol.* 8 (1) (2002) 1–6.
- [10] H. Zhai, H. Maibach, Effects of skin occlusion on percutaneous absorption: an overview, *Skin Pharmacol. Appl.* 14 (2001) 1–10.
- [11] S. Björklund, J. Engblom, K. Thuresson, E. Sparr, A water gradient can be used to regulate drug transport across skin, *J. Control. Release* 143 (2010) 191–200.
- [12] E. Sparr, H. Wennerström, Responding phospholipid membranes-interplay between hydration and permeability, *Biophys. J.* 81 (2) (2001) 1014–1028.
- [13] S. Björklund, A. Nowacka, J.A. Bouwstra, E. Sparr, D. Topgaard, Characterization of stratum corneum molecular dynamics by natural-abundance <sup>13</sup>C solid-state NMR, *PLoS One* 8 (4) (2013) e61889.
- [14] S. Björklund, T. Ruzgas, A. Nowacka, I. Dahi, D. Topgaard, E. Sparr, J. Engblom, Skin membrane electrical impedance properties under the influence of a varying water gradient, *Biophys. J.* 104 (12) (2013) 2639–2650.
- [15] H. Schaefer, T.E. Redelmeier, Structure and dynamics of the skin barrier, in: *Skin Barrier: Principles of Percutaneous Absorption*, Karger, 1996, pp. 1–42.
- [16] J. Levin, R. Miller, A guide to the ingredients and potential benefits of over-the-counter cleansers and moisturizers for rosacea patients, *J. Clin. Aesthet. Dermatol.* 4 (8) (2011) 31–49.
- [17] S. Björklund, J. Engblom, K. Thuresson, E. Sparr, Glycerol and urea can be used to increase skin permeability in reduced hydration conditions, *Eur. J. Pharm. Sci.* 50 (5) (2013) 638–645.
- [18] S. Björklund, J.M. Andersson, Q.D. Pham, A. Nowacka, D. Topgaard, E. Sparr, Stratum corneum molecular mobility in the presence of natural moisturizers, *Soft Matter* 10 (25) (2014) 4535–4546.
- [19] A.V. Rawlings, C.R. Harding, Moisturization and skin barrier function, *Dermatol. Ther.* 17 (Suppl. 1) (2004) 43–48.
- [20] M. Loden, A.C. Andersson, C. Anderson, I.M. Bergbrant, T. Frodin, H. Ohman, M. H. Sandstrom, T. Sarnhult, E. Voog, B. Stenberg, E. Pawlik, A. Preisler-Haggqvist, A. Svensson, M. Lindberg, A double-blind study comparing the effect of glycerin and urea on dry, eczematous skin in atopic patients, *Acta Derm. Venereol.* 82 (1) (2002) 45–47.
- [21] M. Breternitz, D. Kowatzki, M. Langenauer, P. Elsner, J.W. Fluhr, Placebo-controlled, double-blind, randomized, prospective study of a glycerol-based emollient on eczematous skin in atopic dermatitis: Biophysical and clinical evaluation, *Skin Pharmacol. Physiol.* 21 (1) (2008) 39–45.
- [22] D.W. Osborne, Diethylene glycol monoethyl ether: an emerging solvent in topical dermatology products, *J. Cosmet. Dermatol.* 10 (4) (2011) 324–329.
- [23] F.B. Camargo Jr., L.R. Gaspar, P.M.B.G. Maia Campos, Skin moisturizing effects of panthenol-based formulations, *J. Cosmet. Sci.* 62 (4) (2011) 361–369.
- [24] W. Gehring, M. Gloor, Effect of topically applied dexpanthenol on epidermal barrier function and stratum corneum hydration – results of a human in vivo study, *Arznei. Forschung Drug Res.* 50 (7) (2000) 659–663.
- [25] F. Ebner, A. Heller, F. Rippke, I. Tausch, Topical use of dexpanthenol in skin disorders, *Am. J. Clin. Dermatol.* 3 (6) (2002) 427–433.
- [26] M.E. Lane, Skin penetration enhancers, *Int. J. Pharm.* 447 (1–2) (2013) 12–21.
- [27] A.L. Vangeet, Calibration of methanol nuclear magnetic resonance thermometer at low temperature, *Anal. Chem.* 42 (6) (1970) 679–680.
- [28] A. Pines, J.S. Waugh, M.G. Gibby, Proton enhanced nuclear induction spectroscopy – method for high-resolution NMR of dilute spins in solids, *J. Chem. Phys.* 56 (4) (1972) 1776–1777.
- [29] G.A. Morris, R. Freeman, Enhancement of nuclear magnetic resonance signals by polarization transfer, *J. Am. Chem. Soc.* 101 (3) (1979) 760–762.
- [30] A. Nowacka, N. Bongartz, O.H.S. Ollila, T. Nylander, D. Topgaard, Signal intensities in <sup>1</sup>H-<sup>13</sup>C CP and INEPT MAS NMR of liquid crystals, *J. Magn. Reson.* 230 (2013) 165–175.
- [31] A. Nowacka, P.C. Mohr, J. Norrman, R.W. Martin, D. Topgaard, Polarization transfer solid-state NMR for studying surfactant phase behavior, *Langmuir* 26 (22) (2010) 16848–16856.
- [32] A.E. Bennett, C.M. Rienstra, M. Auger, K.V. Lakshmi, R.G. Griffin, Heteronuclear decoupling in rotating solids, *J. Chem. Phys.* 103 (1995) 6951–6958.
- [33] L. Chen, Z. Weng, L. Goh, M. Garland, An efficient algorithm for automatic phase correction of NMR spectra based on entropy minimization, *J. Magn. Reson.* 158 (2002) 164–168.
- [34] J.D. van Beek, MatNMR: a flexible toolbox for processing, analyzing and visualizing magnetic resonance data in Matlab, *J. Magn. Reson.* 187 (2007) 19–26.
- [35] R.L. Bronaugh, R.F. Stewart, Methods for in vitro percutaneous absorption studies. IV: The flow-through diffusion cell, *J. Pharm. Sci.* 74 (1) (1985) 64–67.
- [36] H. Clowes, R. Scott, J. Heylings, Skin absorption: flow-through or static diffusion cells, *Toxic. in Vitro* 8 (1994) 827–830.
- [37] S.D. Campbell, K.K. Kranning, E.G. Schibli, S.T. Momii, Hydration characteristics and electrical-resistivity of stratum-corneum using a noninvasive 4-point microelectrode method, *J. Invest. Dermatol.* 69 (3) (1977) 290–295.
- [38] J.D. DeNuzzio, B. Berner, Electrochemical and iontophoretic studies of human skin, *J. Control. Release* 11 (1–3) (1990) 105–112.
- [39] D. Foley, J. Corish, O.I. Corrigan, Iontophoretic delivery of drugs through membranes including human stratum corneum, *Solid State Ionics* 53–56 (Part 1) (1992) 184–196.
- [40] B. Hirschorn, M.E. Orazem, B. Tribollet, V. Vivier, I. Frateur, M. Musiani, Determination of effective capacitance and film thickness from constant-phase-element parameters, *Electrochim. Acta* 55 (21) (2010) 6218–6227.
- [41] Y.N. Kalia, R.H. Guy, The electrical characteristics of human skin in vivo, *Pharm. Res.* 12 (11) (1995) 1605–1613.
- [42] A.H. Lackermeier, E.T. McAdams, G.P. Moss, A.D. Woolfson, In vivo ac impedance spectroscopy of human skin: theory and problems in monitoring of passive percutaneous drug delivery, *Ann. New York Acad. Sci.* 873 (1999) 197–213 (*Electrical Bioimpedance Methods*).
- [43] K. Kontturi, L. Murtomaki, Impedance spectroscopy in human skin. A refined model, *Pharm. Res.* 11 (9) (1994) 1355–1357.
- [44] M.E. Orazem, N. Pebere, B. Tribollet, Enhanced graphical representation of electrochemical impedance data, *J. Electrochem. Soc.* 153 (4) (2006) B129–B136.
- [45] H. Schaefer, T.E. Redelmeier, Composition and structure of the stratum corneum, in: *Skin Barrier: Principles of Percutaneous Absorption*, Karger, 1996, pp. 43–86.
- [46] P.W. Wertz, D.T. Downing, Ceramides of pig epidermis – structure determination, *J. Lipid Res.* 24 (6) (1983) 759–765.
- [47] W.L. Earl, D.L. VanderHart, Observations in solid polyethylenes by carbon-13 magnetic resonance with magic angle sample spinning, *Macromolecules* 12 (1979) 762–767.
- [48] A. Alonso, N.C. Meirelles, M. Tabak, Effect of hydration upon the fluidity of intercellular membranes of stratum corneum: an EPR study, *BBA-Biomembranes* 1237 (1) (1995) 6–15.
- [49] C.L. Silva, D. Topgaard, V. Kocherbitov, J.J.S. Sousa, A.A.C.C. Pais, E. Sparr, Stratum corneum hydration: phase transformations and mobility in stratum corneum, extracted lipids and isolated corneocytes, *Biochim. Biophys. Acta* 1768 (2007) 2647–2659.
- [50] O. Soubias, F. Jolibois, V. Reat, A. Milon, Understanding sterol-membrane interactions. Part II: Complete H-1 and C-13 assignments by solid-state NMR spectroscopy and determination of the hydrogen-bonding partners of cholesterol in a lipid bilayer, *Chem. Eur. J.* 10 (23) (2004) 6005–6014.
- [51] J. Tsai, P. Hung, H. Sheu, Molecular weight dependence of polyethylene glycol penetration across acetone-disrupted permeability barrier, *Arch. Dermatol. Res.* 293 (2001) 302–307.
- [52] C. Albér, B.D. Brandner, S. Björklund, P. Billsten, R.W. Corkery, J. Engblom, Effects of water gradients and use of urea on skin ultrastructure evaluated by confocal Raman microspectroscopy, *BBA-Biomembranes* 1828 (11) (2013) 2470–2478.

- [53] D.M. LeNeveu, R.P. Rand, V.A. Parsegian, Measurement of forces between lecithin bilayers, *Nature* 259 (5544) (1976) 601–603.
- [54] F.O. Costa-Balogh, H. Wennerström, L. Wadsö, E. Sparr, How small polar molecules protect membrane systems against osmotic stress: the urea-water-phospholipid system, *J. Phys. Chem. B* 110 (47) (2006) 23845–23852.
- [55] A. Nowacka, S. Douezan, L. Wadsö, D. Topgaard, E. Sparr, Small polar molecules like glycerol and urea can preserve the fluidity of lipid bilayers under dry conditions, *Soft Matter* 8 (5) (2012) 1482–1491.
- [56] W.H.M.C.v. Hinsberg, J.C. Verhoef, H.E. Junginger, H.E. Bodde, Thermoelectrical analysis of the human skin barrier, *Thermochim. Acta* 248 (1995) 303–318.
- [57] Y.N. Kalia, F. Pirot, R.H. Guy, Homogeneous transport in a heterogeneous membrane: water diffusion across human stratum corneum in vivo, *Biophys. J.* 71 (5) (1996) 2692–2700.
- [58] S.Y. Oh, L. Leung, D. Bommannan, R.H. Guy, R.O. Potts, Effect of current, ionic strength and temperature on the electrical properties of skin, *J. Control. Release* 27 (2) (1993) 115–125.
- [59] I. Iwai, H. Han, L.d. Hollander, S. Svensson, L.-G. Ofverstedt, J. Anwar, J. Brewer, M. Bloksgaard, A. Lalouef, D. Nosek, S. Masich, L.A. Bagatolli, U. Skoglund, L. Norlen, The human skin barrier is organized as stacked bilayers of fully extended ceramides with cholesterol molecules associated with the ceramide sphingoid moiety, *J. Invest. Dermatol.* 132 (9) (2012) 2215–2225.
- [60] J.A. Bouwstra, G.S. Gooris, W. Bras, D.T. Downing, Lipid organization in pig stratum corneum, *J. Lipid Res.* 36 (4) (1995) 685–695.
- [61] E. Sparr, D. Millecamps, M. Isoir, V. Burnier, A. Larsson, B. Cabane, Controlling the hydration of the skin through the application of occluding barrier creams, *J. R. Soc. Interface* 10 (80) (2013).
- [62] J.E. Harrison, A.C. Watkinson, D.M. Green, J. Hadgraft, K. Brain, The relative effect of Azone(R) and Transcutol(R) on permeant diffusivity and solubility in human stratum corneum, *Pharm. Res.* 13 (4) (1996) 542–546.
- [63] R. Panchagnula, W.A. Ritschel, Development and evaluation of an intracutaneous depot formulation of corticosteroids using transcutol as a cosolvent – in vitro, ex vivo and in vivo rat studies, *J. Pharm. Pharmacol.* 43 (9) (1991) 609–614.
- [64] R. Censi, V. Martena, E. Hoti, L. Malaj, P. Di Martino, Permeation and skin retention of quercetin from microemulsions containing Transcutol (R) P, *Drug Dev. Ind. Pharm.* 38 (9) (2012) 1128–1133.